

TERNARY FISSION OF ^{252}Cf WITHIN THE LIQUID DROP MODEL

V. MIRZAEI, H. MIRI-HAKIMABAD

Physics Department, Faculty of science, Ferdowsi University of Mashhad,
P.O. BOX 91775-1436, Mashhad, Iran,
E-mail: va_mi950@stu-mail.um.ac.ir, mirihakim@ferdowsi.um.ac.ir

Received August 30, 2011

Abstract. A nuclear shape parameterization that leads to the formation of three co-linear fragments was used to investigate the ternary fission. The deformation energy was computed within the liquid drop model in the framework of the Yukawa-plus-exponential model. The ternary fission barrier was estimated by taking into account deformation dependent terms as the volume energy, the Coulomb energy, and the surface energy. The trajectory after the scission of the ternary system was computed by solving twelve differential motion equations related to the motion. Finally the penetrability for binary and ternary processes was compared.

Key words: ternary fission, fission barrier, effective mass.

1. INTRODUCTION

Fission is a binary process, in which two particles of comparable mass (the primary fission fragments) are formed after the splitting of the parent nucleus. Much less frequently, more than two particles are formed and if precisely three particles appear, the fission event is classified as a ternary event. A ternary fission process occurs once every few hundred of fission events. Roughly speaking, about 25% more ternary fission is present in spontaneous fission compared to the same fissioning system formed after thermal neutron capture. The most important light-charge-particle accompanied in the process of ternary fission is alpha-particle [1–5], indeed about 90% of the ternary particles are alpha-particles and about 10% tritons, the remaining fraction being constituted by a large variety of particles. In this sense, small traces of emission of light-charge-particles like isotopes of H, He, Be were observed in the spontaneous ternary fission of ^{252}Cf [6,7,8,9].

The energy spectrum of the alpha-particle stemming out in ternary fission is very long and is ranging from 6 to 38 MeV [6,10,11]. Such energetic of alpha-particles have long range which differs from the less energetic short-range alpha-particles emitted from the radioactive alpha-decay [12].

As evidenced by the experimental angular distribution, the light ternary particles are emitted about perpendicular to the fission axis. This represents an indication that the light particle is formed in the median region between the heavy

fragments. In this work we used nuclear shape parameterization [13] appropriate for the investigation of the ternary fission and computed the fission barrier and the dynamical path after the scission. The fission barrier is obtained within the liquid drop model in the framework of the Yukawa-plus-exponential extended for ternary systems with different charge densities. In the present work we considered only the case with reflection symmetry. That is the two heavier fragments are the same. Due to the fact that light beta-stable nuclei have the same number of protons and neutrons $Z_l=N_l$ (the “l” represents light-charge-particle or middle fragment) and in heavy nuclei $Z_h<N_h$ (the “h” represents heavy or outer fragments) it is important to consider the difference between mass- and charge-asymmetry parameters:

$$\begin{aligned}\eta_A &= (A_h - A_l)/(A_h + A_l), \\ \eta_Z &= (Z_h - Z_l)/(Z_h + Z_l).\end{aligned}\quad (1)$$

To obtain the fission barrier, a trajectory in our configuration space is chosen in such a way that the total deformation energy is minimized.

2. NUCLEAR SHAPE PARAMETRIZATION

In nuclear fission studies, we are interested in using a nuclear shape parameterization which contains the least possible number of generalized coordinates but gives a reasonable description of the equilibrium shapes. For this purpose, in order to obtain three co-linear spherical fragments we use the model that Mignen *et al.* [13]. The surface equation with an azimuthally symmetry around the z axis is:

$$x^2 = -z^2 + \frac{1}{2}s_i^2c_i^2 + \frac{1}{2}c_i \left[4(1-s_i^2)z^2 + s_i^4c_i^2 \right]^{1/2} \begin{cases} i=1 & \text{for } z > 0 \\ i=2 & \text{for } z < 0. \end{cases} \quad (2)$$

The parameters can be identified in Fig. 1.

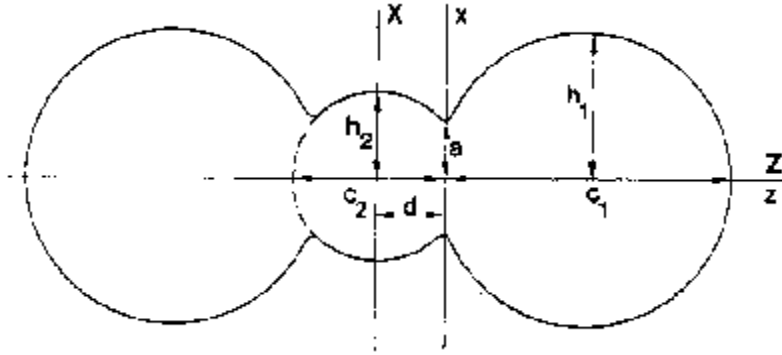


Fig. 1 – Nucleus surface shape according Eq. 2.

In this equation a is the neck radius, c_1 and c_2 are the lengths of fragments. Assuming volume conservation during the deformation, the two dimensionless parameters $s_1=a/c_1$, and $s_2=a/c_2$ are sufficient to define the shape completely. To connect s_1 and s_2 with the final asymmetry between the central fragment and the two other external identical fragments, the following expression has been used,

$$\begin{aligned} s_2^2 &= \frac{s_1^2}{[s_1^2 + (1 - s_1^2) \beta^2]}, \\ c_2^2 &= s_1^2 c_1^2 + (1 - s_1^2) \beta^2 c_1^2, \end{aligned} \quad (3)$$

where $\beta=R_1/R_2$ is the ratio of different radius and in the other word is the deformation parameter. By decreasing s_1 from 1 to 0, the nucleus surface shape piecemeal deforms from a spherical state to three tangent spherical fragments. The parameter d is obtained from the equation below [13]

$$d = \begin{cases} 0.5 c_2 [(1 - 2s_2^2)/(1 - s_2^2)]^{1/2} & \text{for } 0 \leq s_2 < 1/\sqrt{2} \\ 0 & \text{for } 1/\sqrt{2} \leq s_2 < 1 \end{cases} \quad (4)$$

and h is as follow

$$h_i = \begin{cases} 0.5c_i / (1 - s_i^2)^{1/2} & (i=1,2) \quad \text{for } 0 \leq s_i < 1/\sqrt{2} \\ a & \text{for } 1/\sqrt{2} \leq s_i \leq 1. \end{cases} \quad (5)$$

According to the Eq.(4) one can see that when $0 \leq s_2 < 1/2^{1/2}$ the necks becomes to appear.

3. POTENTIAL ENERGY

In the LDM model, the volume, the surface and the Coulomb energies vary during fission and are deformation dependents. In this section the model used for these three energies will be presented and the formalism will be extended the ternary systems. In the double folded Yukawa-Plus-Exponential potential model, the surface energy is replaced by double folded Yukawa-Plus-Exponential potential energy as follow[14,15,16]

$$E_Y = -\frac{a_2}{8\pi^2 r_0^2 a^4} \int \int_{v_n} \left(\frac{r_{12}}{a} - 2 \right) \frac{\exp(-r_{12}/a)}{r_{12}/a} d^3 r_1 d^3 r_2, \quad (6)$$

where $r_{12}=|\mathbf{r}_1-\mathbf{r}_2|$, a is the diffusivity parameter, and r_0 is the sharp-surface parameter. The six fold integral is taken over the volume v_n (nucleus volume). For a spherical shape, Eq. (6) leads to

$$E_{Y0} = a_2 A^{2/3} \left\{ 1 - 3 \left(\frac{a}{R_0} \right)^2 + \left(1 + \frac{R_0}{a} \right) \left[2 + 3 \frac{a}{R_0} \left(1 + \frac{a}{R_0} \right) \right] \exp \left(-\frac{2R_0}{a} \right) \right\} \quad (7)$$

and the variation of the surface energy to respect to the spherical shape is as follow

$$\delta E_S = E_Y - E_{Y0}. \quad (8)$$

As we know the Coulomb energy of a volume v_n is obtained from the following equation

$$E_c = \frac{1}{2} \int \int_{v_n} \frac{\rho_e(\vec{r}_1) \rho_e(\vec{r}) d^3 r_1 d^3 r}{|\vec{r} - \vec{r}_1|}. \quad (9)$$

Integrating of Eq. (9) over a sphere with uniform charge density we obtain the relation

$$E_{c0} = 3e^2 Z^2 / (5r_0 A^{1/3}), \quad (10)$$

where e is the electric charge of proton and A is mass number of nucleus. Therefore the variation of Coulomb energy with respect the spherical shape is

$$\delta E_c = E_c - E_{c0}. \quad (11)$$

Volume conservation is a consequence of the low compressibility of nuclear matter. Finally, the fact that the charge asymmetry is a varying quantity during the fission process leads us to take into consideration a variation of the volume energy as follows:

$$\begin{aligned} \delta E_V &= E_{V2} + 2E_{V1} - E_{V0} \neq 0, \\ E_{Vi} &= -a_i A_i, \\ a_{i1} &= a_V (1 - \chi_V I_i)^2, \\ I_i &= (N_i - Z_i) / A_i, \end{aligned} \quad (12)$$

where $a_V = 15.9927$ MeV, $\chi_V = 1.927$, and we denoted the volume of each outer fragments plotted in Fig.1 with V_1 and middle one with V_2 .

To characterize the formation of three fragments, we extended the formalism developed for binary fission [15] in order to treat the ternary fission. So, the surface energy becomes

$$\begin{aligned}
E_Y = & -\frac{4a_{21}}{8\pi^2 r_0^2 a^4} \int_{V_1} d^3 r_1 \int_{V_1} \left(\frac{r_{12}}{a} - 2 \right) \frac{\exp(-r_{12}/a)}{r_{12}/a} d^3 r_1 d^3 r_2 - \\
& -\frac{4\sqrt{a_{21}a_{22}}}{8\pi^2 r_0^2 a^4} \int_{V_1} d^3 r_1 \int_{V_2} \left(\frac{r_{12}}{a} - 2 \right) \frac{\exp(-r_{12}/a)}{r_{12}/a} d^3 r_1 d^3 r_2 - \\
& -\frac{a_{22}}{8\pi^2 r_0^2 a^4} \int_{V_2} d^3 r_1 \int_{V_2} \left(\frac{r_{12}}{a} - 2 \right) \frac{\exp(-r_{12}/a)}{r_{12}/a} d^3 r_1 d^3 r_2,
\end{aligned} \tag{13}$$

where

$$B_Y = \frac{E_Y}{E_{Y0}} = 4 \frac{a_{21}}{a_{20}} B_{Y1} + 4 \frac{\sqrt{a_{21}a_{22}}}{a_{20}} B_{Y12} + \frac{a_{22}}{a_{20}} B_{Y2}. \tag{14}$$

The coulomb energy will be considered as follows:

$$E_c = 2\rho_{1e}^2 \int_{V_1} d^3 r_1 \int_{V_1} \frac{d^3 r_2}{r_{12}} + \frac{1}{2} \rho_{2e}^2 \int_{V_2} d^3 r_1 \int_{V_2} \frac{d^3 r_2}{r_{12}} + 2\rho_{1e}\rho_{2e} \int_{V_1} d^3 r_1 \int_{V_2} \frac{d^3 r_2}{r_{12}}, \tag{15}$$

where

$$B_c = \frac{E_c}{E_{c0}} = 4 \left(\frac{\rho_{1e}}{\rho_{oe}} \right)^2 B_{c1} + 4 \frac{\rho_{1e}\rho_{2e}}{\rho_{oe}} B_{c12} + \left(\frac{\rho_{2e}}{\rho_{oe}} \right)^2 B_{c2}. \tag{16}$$

The parameters of Eq.(14) are calculated with the following relations

$$B_{Y1} = b_Y \int_{-1}^{z_1} dz \int_{-1}^{z_1} dz' \int_0^1 dw F_1 F_2 Q_Y, \tag{17}$$

$$B_{Y12} = b_Y \int_{-1}^{z_1} dz \int_{z_1}^{z_2} dz' \int_0^1 dw F_1 F_2 Q_Y, \tag{18}$$

$$B_{Y2} = b_Y \int_{z_1}^{z_2} dz \int_{z_1}^{z_2} dz' \int_0^1 dw F_1 F_2 Q_Y, \tag{19}$$

where

$$\begin{aligned}
b_Y &= -d_1^4 (r_0 / 2a^2) a_2 R_0 A / E_{Y0} \quad ; \quad d_1 = (z_0'' - z_0') / (2R_0); \\
F_1 &= X^2(z) - X(z)X_1(z') \cos \varphi - \frac{1}{2}(z - z') \frac{dX^2(z)}{dz}; \\
F_2 &= X_1^2(z') - X_1(z')X(z) \cos \varphi + \frac{1}{2}(z - z') \frac{dX_1^2(z')}{dz'}; \\
Q_Y &= [P^{1/2} - 2a / R_0 d_1 + (P^{1/2} + 2a / R_0 d_1) \exp(-R_0 d_1 P^{1/2} / a)] / P^2; \\
P &= X^2(z) + X_1^2(z') - 2X(z)X_1(z') \cos(\varphi) + (z - z')^2; \quad \varphi = 2\pi w.
\end{aligned}$$

X, X_1 are the equations of nuclear surface shape renormalized such that -1 and 1 represents the end sides of the nucleus. Therefore, -1 and 1 correspond to $(-c_1-d)$ and (c_1+d) , respectively, while z_1, z_2 correspond to $-d, d$ respectively in the renormalized representation. Furthermore, z_0'', z_0' , correspond to $(c_1+d), (-c_1-d)$. R_0 is the radius of the parent nucleus considered spherical.

Also according to the Davies-Sierk method, the terms B_c of Eq.(16) are calculated with the following relationships

$$B_{c1} = b_c \int_{-1}^{z_1} dz \int_{-1}^{z_1} dz' F(z, z'), \quad (20)$$

$$B_{c12} = b_c \int_{-1}^{z_1} dz \int_{z_1}^{z_2} dz' F(z, z'), \quad (21)$$

$$B_{c2} = b_c \int_{z_1}^{z_2} dz \int_{z_1}^{z_2} dz' F(z, z'), \quad (22)$$

where

$$\begin{aligned}
b_c &= 5d_1^5 / 8\pi \\
F(z, z') &= \left\{ X(z)X_1(z') \left[(K - 2D) / 3 \right] \left[2(X^2(z) + X_1^2(z')) \right] - \right. \\
&\quad \left. -(z - z')^2 + \frac{3}{2}(z - z') \left(\frac{dX_1^2(z')}{dz'} - \frac{dX^2(z)}{dz} \right) \right] + \\
&\quad + K \left[X^2(z)X_1^2(z') / 3 + \left(X^2(z) - \frac{1}{2}(z - z') \frac{dX^2(z)}{dz} \right) \cdot \right. \\
&\quad \left. \cdot \left(X_1^2(z') + \frac{1}{2}(z - z') \frac{dX_1^2(z')}{dz'} \right) \right] \left. \right\} a_p^{-1}
\end{aligned}$$

and

$$a_p^2 = (X(z) + X_1(z'))^2 + (z - z')^2; \quad k^2 = 4X(z)X_1(z')/a_p^2.$$

K, K' are the complete elliptic integrals of the first and second kind, respectively.

$$K(k) = \int_0^{\pi/2} (1 - k^2 \sin^2 t)^{-1/2} dt; \quad K'(k) = \int_0^{\pi/2} (1 - k^2 \sin^2 t)^{1/2} dt;$$

$$D = (K - K')/k^2.$$

The previous relations will be used to characterize the ternary fission process.

4. EFFECTIVE MASS AND TRAJECTORY OF THREE FRAGMENTS

A very important step linked to the dynamics of the three particles after the scission. In the case of binary fission the effective mass after the separation is given by the reduced mass and it is simple to compute the action integral. In the case of three particles, the effective mass depends on the position of each particle versus the center of mass of the system, which is on the trajectory. In order to find the trajectory of fission fragments after their separation, one can use of the Euler-Lagrange equations of motion. The Euler-Lagrange equations of motion can be written as

$$L = T - V,$$

$$\frac{d}{dt} \left(\frac{\partial L}{\partial \dot{q}_k} \right) - \frac{\partial L}{\partial q_k} = 0, \quad (23)$$

where T, V are kinetic and potential energy respectively, and q_k are the general coordinates that define the positions of the particles versus the center of mass. In our problem we have three particle which move in a plane (x,y) , so that the unknowns of our system are reduced to six parameters. Therefore $k=1,..6$ and we have six differential equations of second order. One can reduce the order of differential equation from two to one by writing six additional differential equations; finally we have twelve differential equations which give the trajectories of the fragments after separation.

The effective mass of the tripartition can be obtained if the Euler-Lagrange equations of motion are solved. For this purpose we consider that the two heavy fragments have opposite velocities and the light intermediate fragment is at rest.

From considerations linked to the scission time we choose the velocities to range in the interval 10^4-10^6 (fm/fs) [17,18]. Therefore, to fix our initial conditions

we considered that the two heavy fragments are moving in opposite directions with equal velocities while the intermediate alpha particle is at rest. We solved the equations of motion given by Eq. (23).

The effective mass can be written by taking into consideration the components of the tensor of inertia [19] as:

$$M = \sum A_i \left(\left(\frac{\partial x_i}{\partial R} \right)^2 + \left(\frac{\partial y_i}{\partial R} \right)^2 \right), \quad (24)$$

where x_i, y_i are the coordinate of center of i^{th} fragment when the origin located at the center of mother nucleus.

An approximation for the reduced mass can be obtained when the third particle has a very small mass. In these conditions we can neglect the deflection due to the intermediate fragment. In this limiting case the three fragments are collinear and the effective mass can be approximated as:

$$M = A_1 \left(\frac{\partial r_1}{\partial R} \right)^2 + A_2 \left(\frac{\partial r_2}{\partial R} \right)^2 + A_3 \left(\frac{\partial r_3}{\partial R} \right)^2, \quad (25)$$

where R denotes the distance between the two heavy fragments and it is considered as the main coordinate. r_1, r_2, r_3 are distances between the center of mass and centers of the three fragments. As mentioned, this approximation is valid when the mass of the intermediate fragment is much lower than the masses of the heavy ones, and we can write for the external heavy fragments

$$r_1 = \frac{A_3 R}{A_1 + A_3}, \quad (26)$$

and

$$r_3 = \frac{A_1 R}{A_1 + A_3}, \quad (27)$$

so the effective mass will be

$$\begin{aligned} M &= A_1 \left(\frac{A_3}{A_1 + A_3} \right)^2 + A_3 \left(\frac{A_1}{A_1 + A_3} \right)^2 + A_2 \left(\frac{\partial r_2}{\partial R} \right)^2 = \\ &= \frac{A_1 A_3^2 + A_3 A_1^2}{(A_1 + A_3)^2} + A_2 \left(\frac{\partial r_2}{\partial R} \right)^2 = \mu + A_2 \left(\frac{\partial r_2}{\partial R} \right)^2, \end{aligned} \quad (28)$$

then, the mass of the intermediate fragment is small, the effective mass of three fragments will be always greater than the reduced mass of the two heavy fragments

within a quantity that depends on the dynamics of the system. This formalism contradicts an evaluation of the effective mass concerning the ternary fission given by a formula of the type [20]

$$\mu_{123} = \frac{\mu_{12} A_3}{\mu_{12} + A_3} m,$$

$$\mu_{12} = \frac{A_1 A_2}{A_1 + A_2},$$

where m is the nucleon mass. That gives too low values.

5. RESULTS AND DISCUSSION

First of all, a trajectory that connects the parent ground-state up to the formation of three co-linear formed fragments configuration is required. Our nuclear shape parametrization is characterized by two degree of freedom: the mass asymmetry (that fix the mass of the intermediate fragment) and the elongation. The elongation R is defined here as the distance between the centers of the external fragments. Therefore, in Fig. 2 the deformation energy for the parent ^{252}Cf is plotted *versus* these two parameters. using our nuclear shape parametrization. It can be observed that low values of the deformation energy are obtained for configuration with $A_2 = 80$ at the beginning of the fission process, up to an elongation $R = 10$ fm. Afterward, the mass asymmetry change rapidly to reach the final mass asymmetry that correspond to the formation of an alpha particle for $R = 15$ fm.

The family of nuclear shapes obtained along the path corresponding to the minimal energy in the possible configuration space is plotted in Fig. 3. It is interesting to note that up to $R = 12$ fm, the process behaves as a binary fission.

It will be interesting to compare the ternary fission process behavior with that given by the binary one. For this purpose, using the same liquid drop formalism, we investigated the behavior of the binary fission. For binary fission, a parametrization given by two spheres of the same radii smoothly joined within an arc of circle in the median region is used. The median surface gives the neck between the two fragments. This parametrization depends on two generalized coordinates: C the curvature of the neck and R the distance between the centers of the two fragments. This parametrization was widely used in characterization of the fission process [21, 22, 23, 24]. In Fig. 4 we plotted the deformation energy as function of C and R for the binary symmetric fission of ^{252}Cf . The low values of the deformation energy are obtained for small values of C . When the nucleus disintegrates, it starts from the spherical shape and reach a fission valley as indicated by the fission trajectory plotted with a curve in Fig. 4. The shapes obtained along the fission trajectory are plotted in Fig. 5.

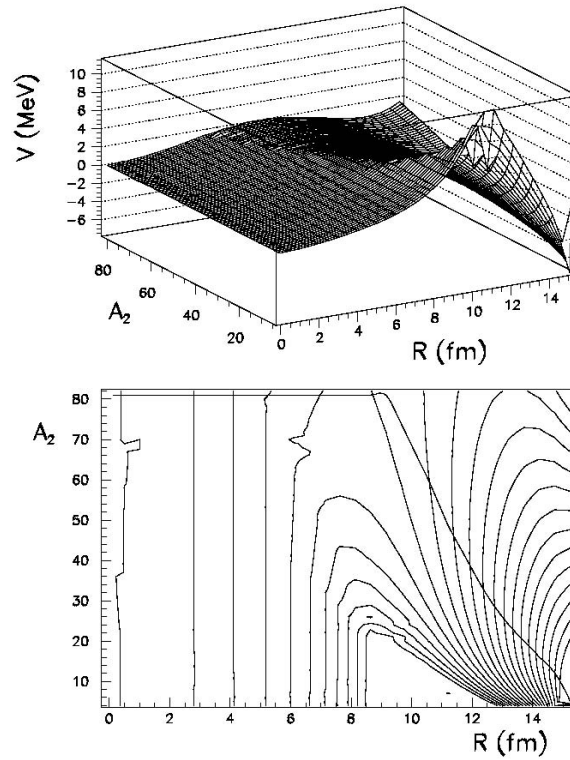


Fig. 2 – Deformation energy as function of the mass of the median fragment A_2 and the elongation parameter R . The best path which minimize energy for ternary fission of ^{252}Cf with alpha emission as light-particle is represented with a thick curve. The step between two equipotential lines is 0.5 MeV.

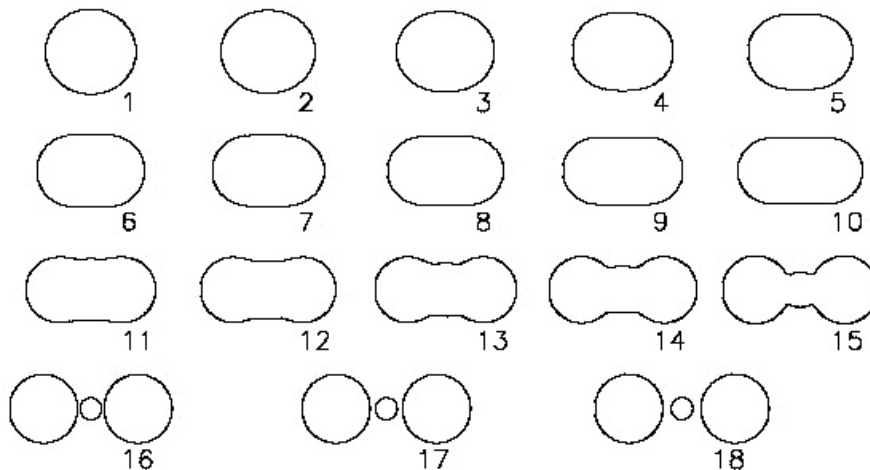


Fig. 3 – Family of shapes obtained along the path that leads to ternary fission with alpha as light-particle. The number below each shape is the distance between center of mass of fragments R in fm.

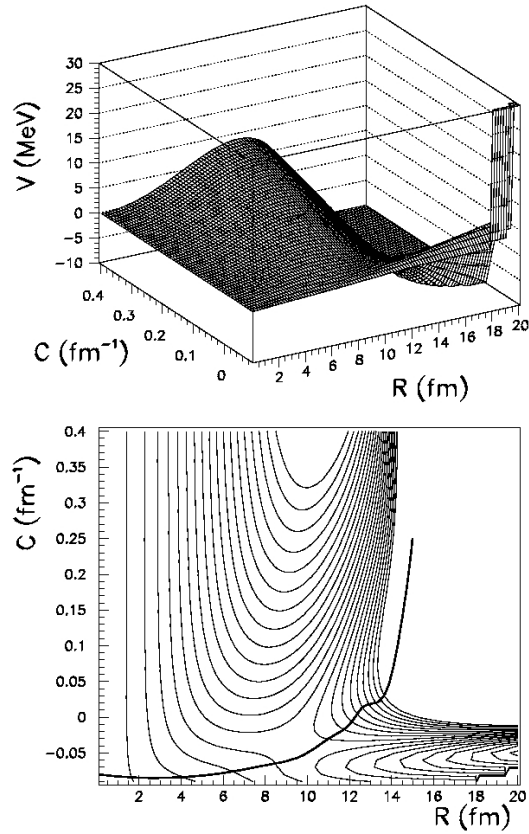


Fig. 4 – Deformation energy as function of the median curvature C and the elongation parameter R . The best path which minimize energy for binary fission of ^{252}Cf is represented with a thick curve. The step between two equipotential lines is 0.5 MeV.

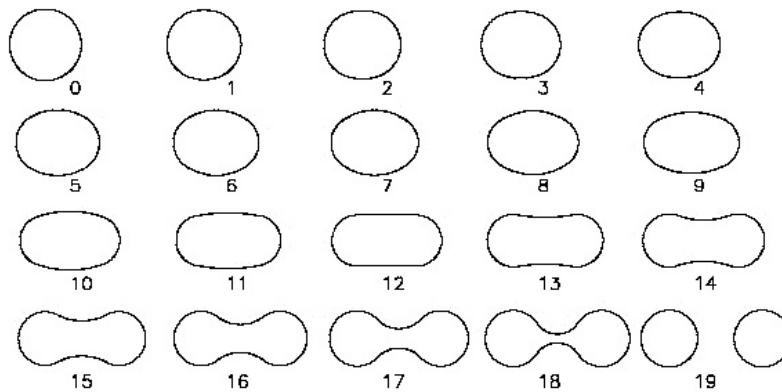


Fig. 5 – Family of shapes obtained along the path that leads to binary fission. The number below each shape is the distance between center of mass of fragments R in fm.

A comparison of the potential barriers obtained for the two modes of fission investigated is made in Fig. 6. As expected, the barrier height of the ternary fission is larger than that of the binary fission. This observation is in line with experimental data that show that the probability to produce a binary fission event is larger than that for a ternary one. Such phenomenon must be also evidenced by calculation of the values of the action integral. By considering that the inertia of the system equals the reduced mass for symmetric fission, we obtained a value of the action integral for ternary process of about 43.07. For binary fission the value of the action integral is 38.24. In this circumstances, the probability for ternary fission is $\exp(38.24)/\exp(43.07)=8\times 10^{-3}$.

The absolute ternary particle emission probability in spontaneous fission of ^{252}Cf is 3.77×10^{-3} [26]. So, our theoretical results are a very good agreement with experimental data.

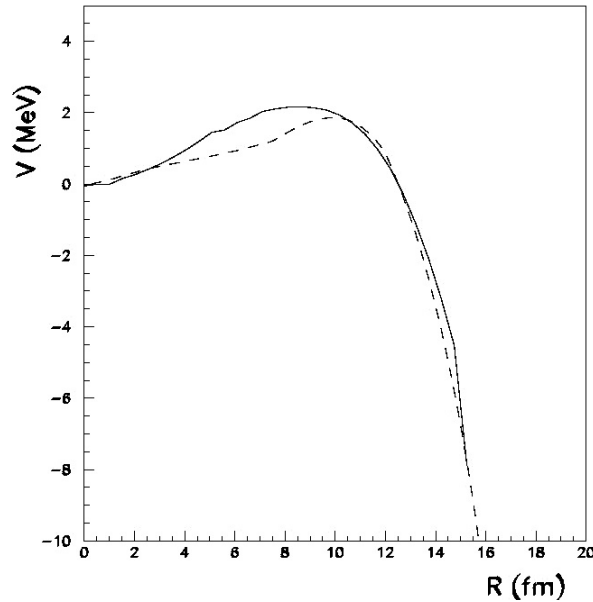


Fig. 6 –Liquid drop fission barriers of ^{252}Cf for binary (symmetry) dashed curve, and ternary fission with alpha emission as light-particle full curve.

After scission, it is important to calculate the trajectory of the three involved fragments using the model discussed in the previous section. This trajectory is represented in Fig. 7. The alpha particle is emitted in a normal direction on the axis that connects the two heavy fission partners. This result is in line within the experimental evidence given by light particle angular distributions of ^{252}Cf given in Ref. [27] where a strongly peaked emission of H, He, Li and Be particles under an angle of about 90° with respect the fission axis was reported. The evaluated inertia

within formula (24) is approximately equal with the reduced mass of the heavy fragments. This property allowed us to compute the action integrals for the two modes within the same inertia.

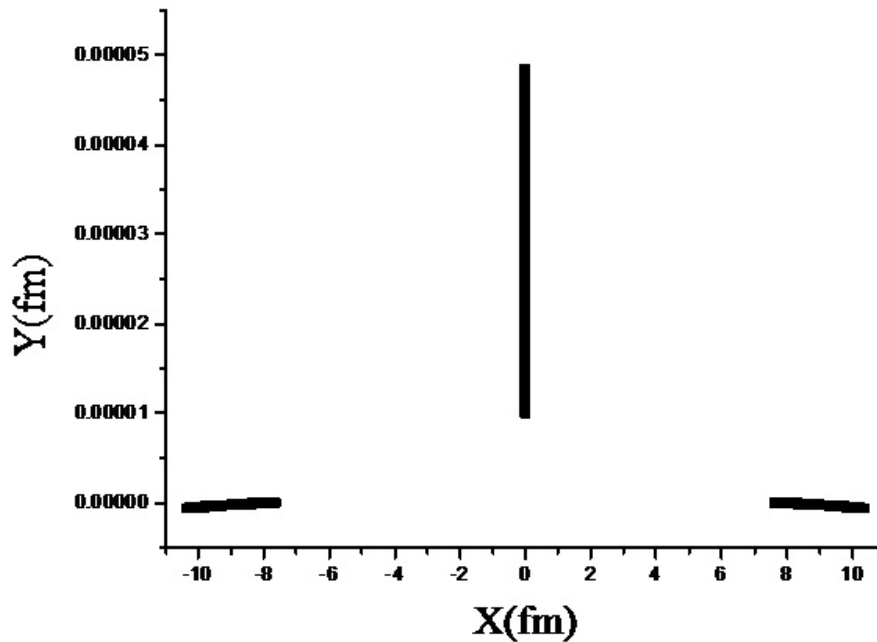


Fig. 7 – Trajectories of fragments for ^{252}Cf ternary fission, the light particle is alpha and it is emitted from the middle.

Acknowledgements. One of us, V.M., acknowledge a Ph.D. grant offered by the Ministry of Science of Iran for a working research stage at the Horia Hulubei National Institute for Physics and Nuclear Engineering. We acknowledge fruitful discussions with Prof. F. Rahimi.

REFERENCES

1. Yu.N. Kopatch, M. Mutterer, D. Schwalm, P. Thirof, F. Gonnenein, Phys. Rev. C, **65**, 044614 (2002).
2. R. Vandenbosch, J. Huizenga, *Nuclear Fission*, Academic Press, New York, 1973.
3. J.F. Wild, P.A. Baisden, R.J. Dougan, E.K. Hulet, R.W. Lougheed, J.H. Landrum, Phys. Rev. C, **32**, 488 (1985).
4. F. Gonnenein, B. Borsig, U. Nast-Linke, S. Neumaier, M. Mutterer, J.P. Theobald, H. Faust, P. Geltenbort, 6th International Conference on *Nuclei Far from Stability* and 9th International Conference on *Atomic Masses and Fundamental Constants*, Bernkastel-Kues, IOP, London, 1989, p. 453.
5. C. Wagemans (Editor), *The Nuclear Fission Process*, CRC Press, Boca Raton, FL, 1991, p. 545.
6. S.W. Cosper, J. Cerny, R.C. Gatti, Phys. Rev., **154**, 1193 (1967).
7. G.M. Raisbeck, T.D. Thomas, Phys. Rev., **172**, 1272 (1968).

8. S.L. Whetstone, T.D. Thomas, Phys. Rev. Lett., **15**, 298 (1965).
9. S.L. Whetstone, T.D. Thomas, Phys. Rev., **154**, 1174 (1967).
10. W. Loveland, Phys. Rev., C, **9**, 395 (1974).
11. V.A. Khriachkov, M.V. Dunaev, I.V. Dunaeva, N.N. Semenova, A.I. Sergachev, Phys. At. Nucl., **67**, 1239 (2004).
12. I. Silisteanu, A.I. Budaca, A.O. Silisteanu, Rom. J. Phys., **55**, 1088 (2010).
13. J. Mignen, G. Royer, J. Phys. G: Nucl. Part. Phys., **16**, L227 (1990).
14. D. N. Poenaru, M. S. Ivascu. *Particle Emission from Nuclei*, Boca Raton, Florida, 1989
15. D. N. Poenaru, M. S. Ivascu, D. Mazilu. Comput. Phys. Commun, **19**, 205, 1980.
16. M. Mirea, O. Bajeat, F. Clapier, F. Ibrahim, A.C, Mueller, N. Pauwels, J. Proust, Eur. Phys. J. A, **11**, 59 (2001).
17. R.W. Hasse, Rep. Prog. Phys., **41**, 1027 (1978).
18. M. Mirea, Phys. Rev. C, **83**, 054608 (2011); Phys. Lett. B, **680**, 316 (2009).
19. M. Mirea, Rom. Rep. Phys., **63**, 676 (2011).
20. K. Manimaran, M. Balasubramaniam. Eur. Phys. J. A, **45**, 293–300 (2010).
21. I. Companis, M. Mirea, A. Isbasescu, Rom. J. Phys., **56**, 63 (2011).
22. M. Mirea, D.S. Delion, A. Sandulescu, Phys. Rev. C, **81**, 044317 (2010); Rom. J. Phys., **55**, 309 (2010).
23. P. Stoica, Rom. Rep. Phys., **63**, 76 (2011).
24. M. Mirea, Phys. Rev. C, **78**, 044618 (2008); Phys. Rev. C, **54**, 302 (1996).
25. M. Mirea, A. Sandulescu, D.S. Delion, Proc. Rom. Acad. Series A, **3**, 203–208 (2011).
26. J. Wild, P. Baisden, R. Dougan, E Hulet, R. Loughheed, Phys. Rev. C, **32**, 488 (1985).
27. C. Wagemans, *Particle Emission from Nuclei*, Vol. III, CRC Press, Boca Raton Florida, 1989.